Science Advances
AAAS

advances.sciencemag.org/cgi/content/full/6/33/eaba3546/DC1

Supplementary Materials for

Bacteria-triggered tumor-specific thrombosis to enable potent photothermal immunotherapy of cancer

Xuan Yi, Hailin Zhou, Yu Chao, Saisai Xiong, Jing Zhong, Zhifang Chai, Kai Yang*, Zhuang Liu*

*Corresponding author. Email: kyang@suda.edu.cn (K.Y.); zliu@suda.edu.cn (Z.L.)

Published 14 August 2020, *Sci. Adv.* **6**, eaba3546 (2020)
DOI: 10.1126/sciadv.aba3546

This PDF file includes:

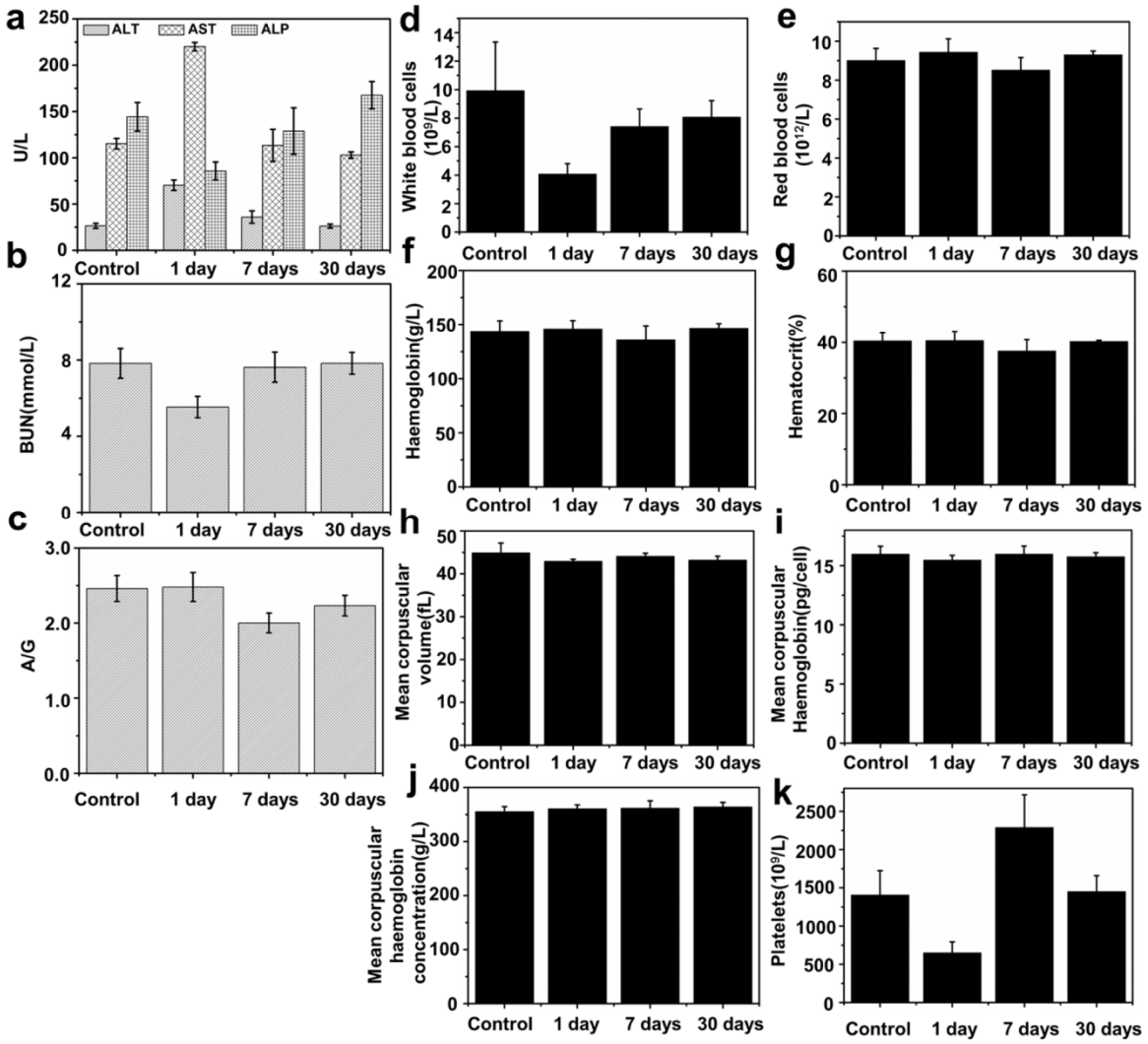

Supporting information Figure S1. **Blood biochemistry and hematology data of healthy female Balb/c mice intravenously (i.v.) injected with *Salmonella* typhimurium ΔppGpp strain at the dose of 5*10^6 CFU per mouse at 1, 7, and 30 d post injection (p.i.).** (a) glutamic-pyruvic transaminase(ALT), alkaline phosphatase (ALP), and aspartate aminotransferase (AST) levels in the blood at various time points after bacteria treatment. (b) Time-course albumin/globin ratios. (c) Blood urea nitrogen (BUN) over time. (d-k) Time-course changes of white blood cells (d), red blood cells (e), hemoglobin (f), hematocrit (g), mean corpuscular volume (h), mean corpuscular hemoglobin (i), mean corpuscular hemoglobin concentration (j), and platelets (k), from control untreated mice and bacteria treated mice. Statistic was based on five mice per data point.

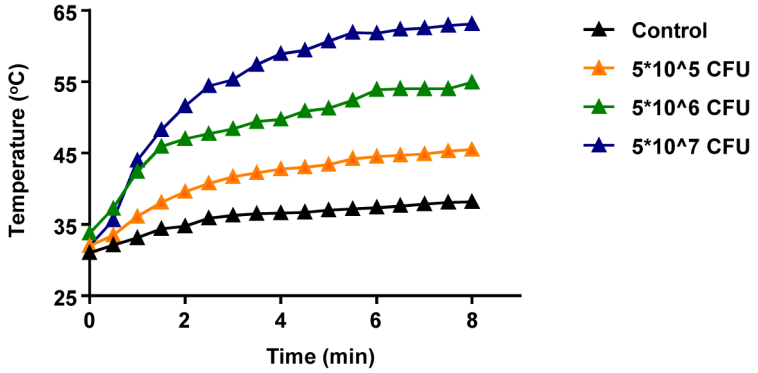

Supporting information Figure S2. The temperature cures of tumors on mice injected with bacteria at the different doses including 5*10^5 CFU, 5*10^6 CFU, 5*10^7 CFU under 808-nm laser irradiation.

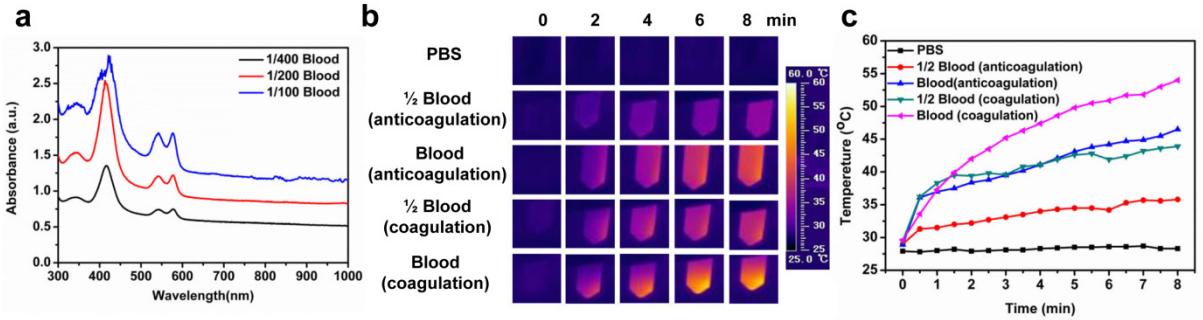

Supporting information Figure S3. The blood absorbance and heating curve under 808-nm laser irradiation. (a) The Uv-Vis absorbanced sprectra of blood samples with different dilutions in phosphate buffered saline (PBS). (b) IR imaging of PBS, coagulated blood and anticoagulated blood under 808-nm laser irradiation at 0.8 W cm^{-2} for 8 min. (c) Change in the maximum temperature of the different samples based on IR thermal imaging date in (b).

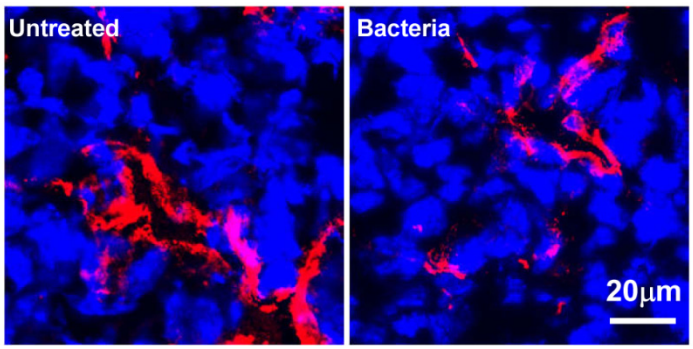

Supporting information Figure S4. The tumor vascular destruction of the mice treated with PBS or bacteria by observing the connectivity of the vascular endothelial cells based on immunofluorescence staining of tumor slices (blue for DAPI staining and red for CD31 staining).

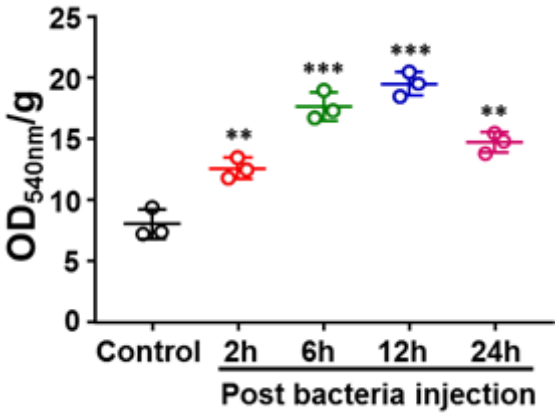

Supporting information Figure S5. **Hemoglobin content in CT26 tumors at different time points after i.v. injection of ΔppGpp strain.** Bars show standard deviations of means. Experiments were repeated three times with identical results.

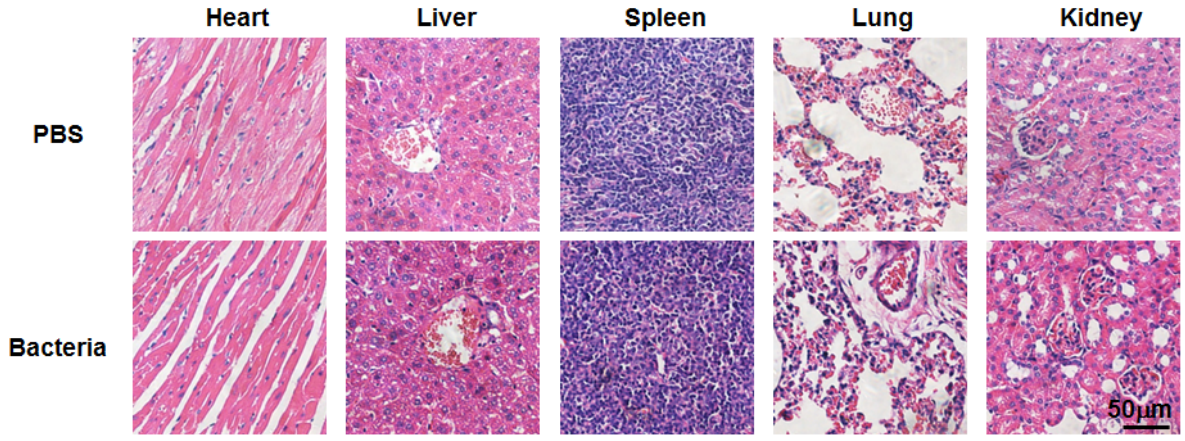

Supporting information Figure S6. Representative images of H&E stained normal organs including heart, liver, spleen, lung and kidney collected from mice injected with PBS or bacteria.

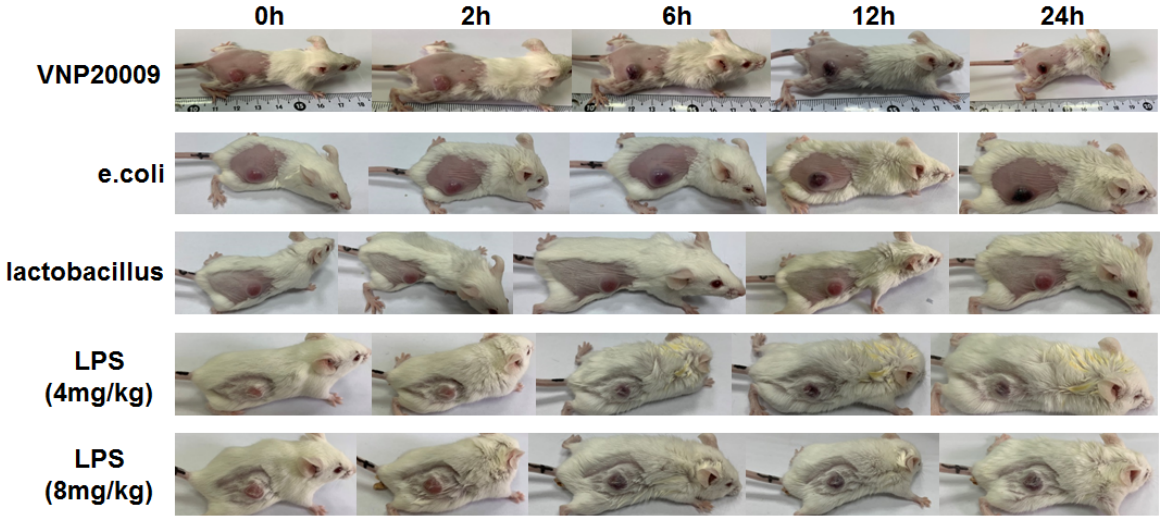

Supporting information Figure S7. Photographs of BALB/c mice before or after injection of bacteria including VNP20009, e.coli and lactobacillus or LPS. Photo Credit: Xuan Yi, Soochow University.

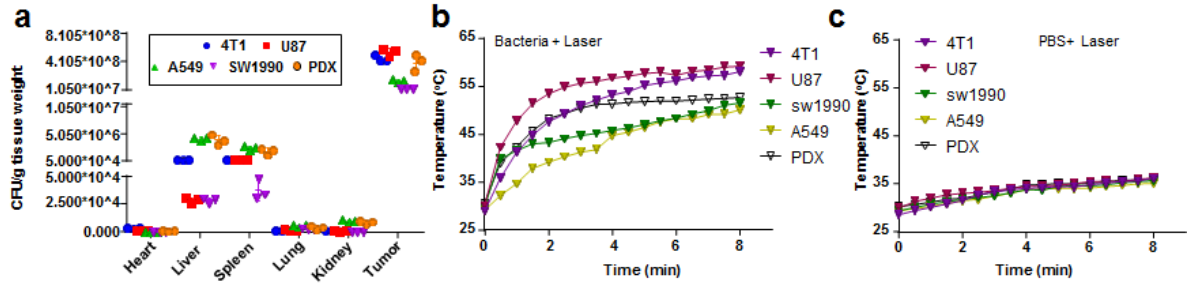

Supporting information Figure S8. Bacterial colonization in various organs of mice and the heating curve of tumor under 808-nm laser irradiation. (a). Bacterial colonization in various organs of mice bearing 4T1 tumors, U87MG tumors, A549 tumors, SW1990 tumors or PDX tumors at 24 h post injection. (b). The temperature changes of different types of tumors on mice injected with bacteria at the dose of $5*10^6$ CFU under 808-nm laser irradiation. (c). The temperature changes of different types of tumors on mice injected with PBS under 808-nm laser irradiation.

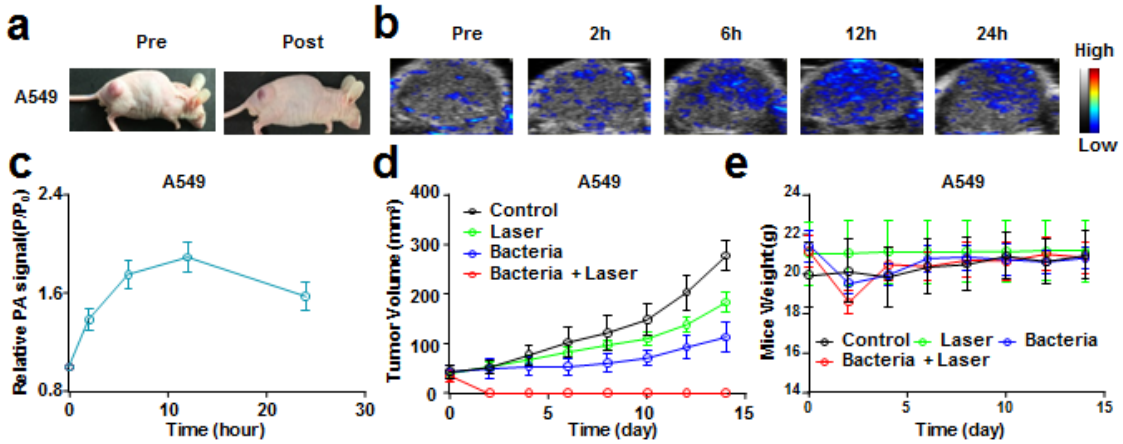

Supporting information Figure S9. Bacteria triggered photothermal ablation of A549 tumors on mice. (a) Photographs of BALB/c mice bearing A549 tumors, before and after injection of bacteria at the dose of $5*10^6$ CFU. Photo Credit: Xuan Yi, Soochow University. (b) Representative photoacoustic images of A549 tumor on mice injected with bacteria at the dose of $5*10^6$ CFU. (c) Quantification of relative photoacoustic signals of tumors on mice injected with $5*10^6$ CFU of bacteria. Data are presented as the mean ±S.D. (d) Tumor growth curves of mice bearing A549 tumors with different treatments indicated. Five mice were used for each group. Data are presented as the mean ±S.E.M. (e) Average body weights of mice-bearing A549 tumor after different treatments indicated.

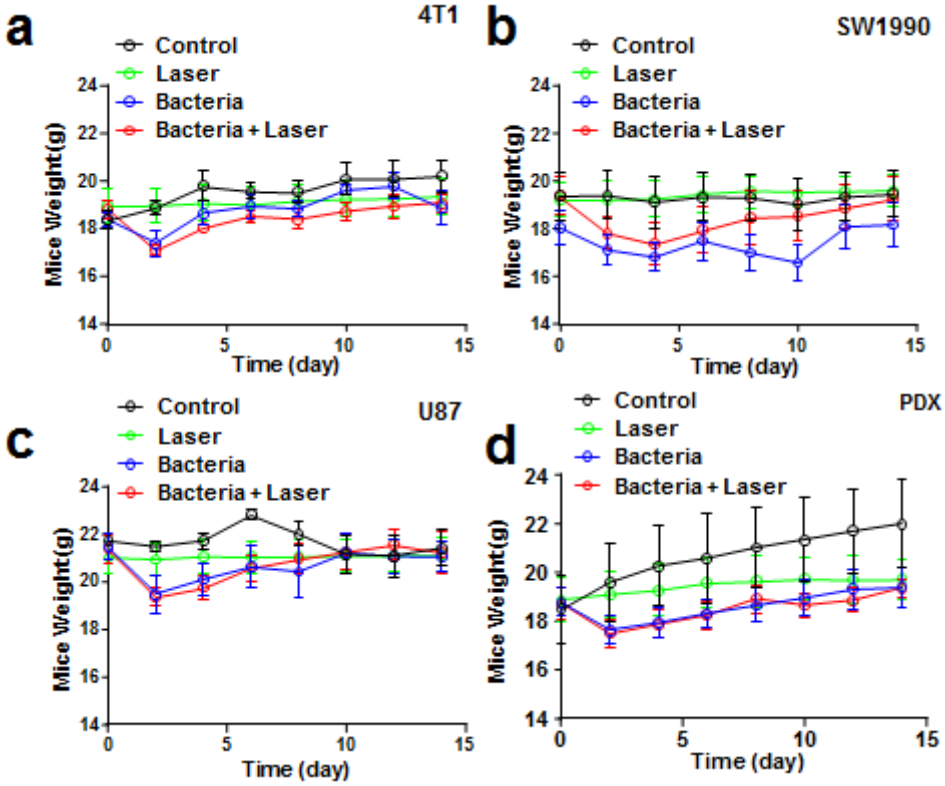

Supporting information Figure S10. Average body weights of mice-bearing 4T1 tumors (a), SW1990 tumors (b), U87MG tumors (c) and PDX tumors (d) after different treatments including PBS injection, bacteria injection at dose of $5*10^6$ CFU and bacteria injection plus 808-nm laser irradiation.

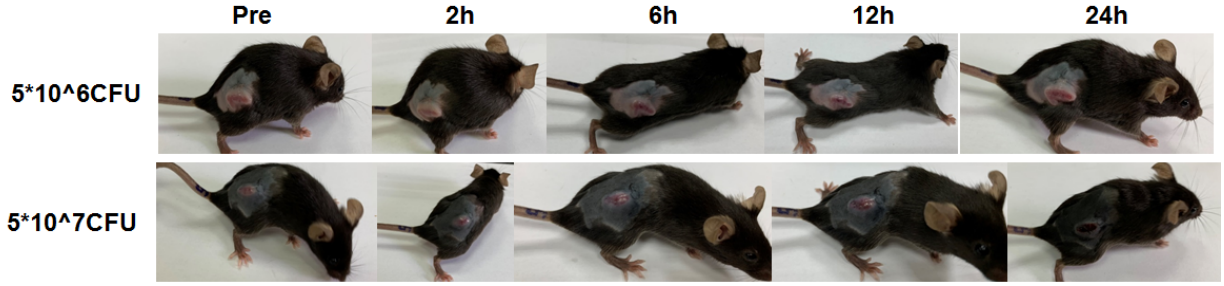

Supporting information Figure S11. Photographs of C57BL/6 mice before or after injection of bacteria at the doses of $5*10^6$ CFU and $5*10^7$ CFU. Photo Credit: Xuan Yi, Soochow University.

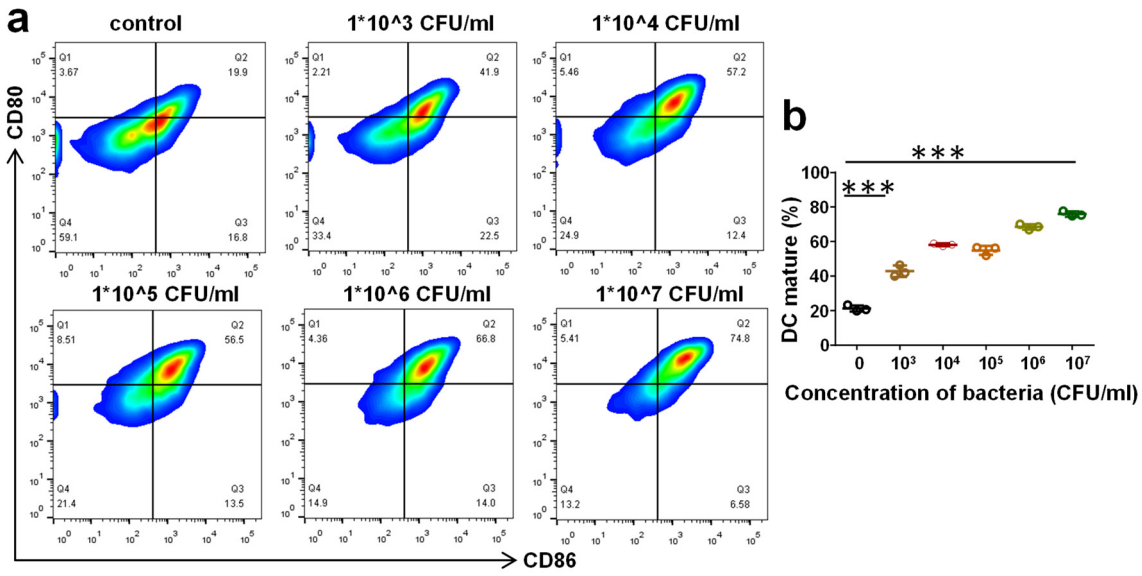

Supporting information Figure S12. (a&b) Representative flow cytometry plots (a) and quantification (b) of in vitro DC maturation induced by different concentrations of heat-treated bacteria obtained after heat treatment for 15 min. DCs maturation was assessed by flow cytometry after staining with CD11c, CD80 and CD86.

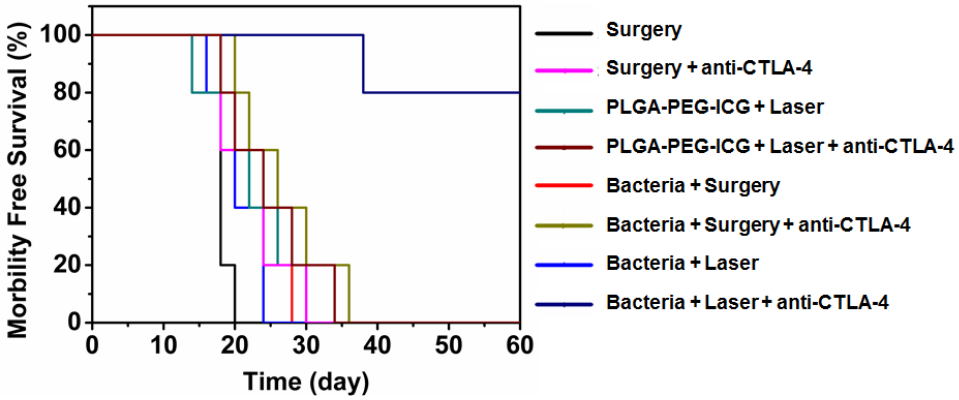

Supporting information Figure S13. Morbidity-free survival of different groups of mice-bearing CT26 tumors after various treatments (five mice per group).

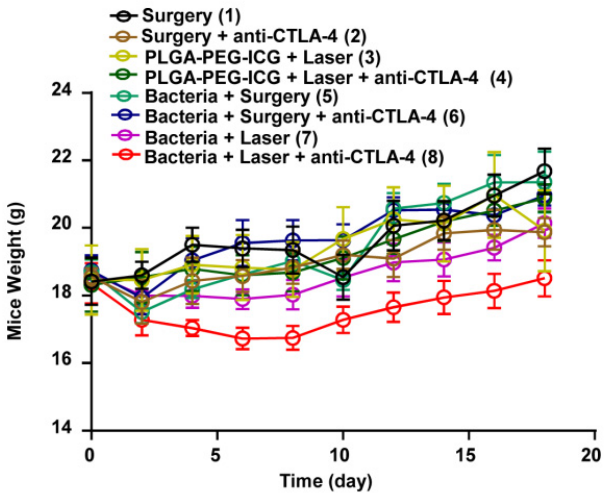

Supporting information Figure S14. Average body weights of mice after various treatments indicated. Five mice were used in each group.

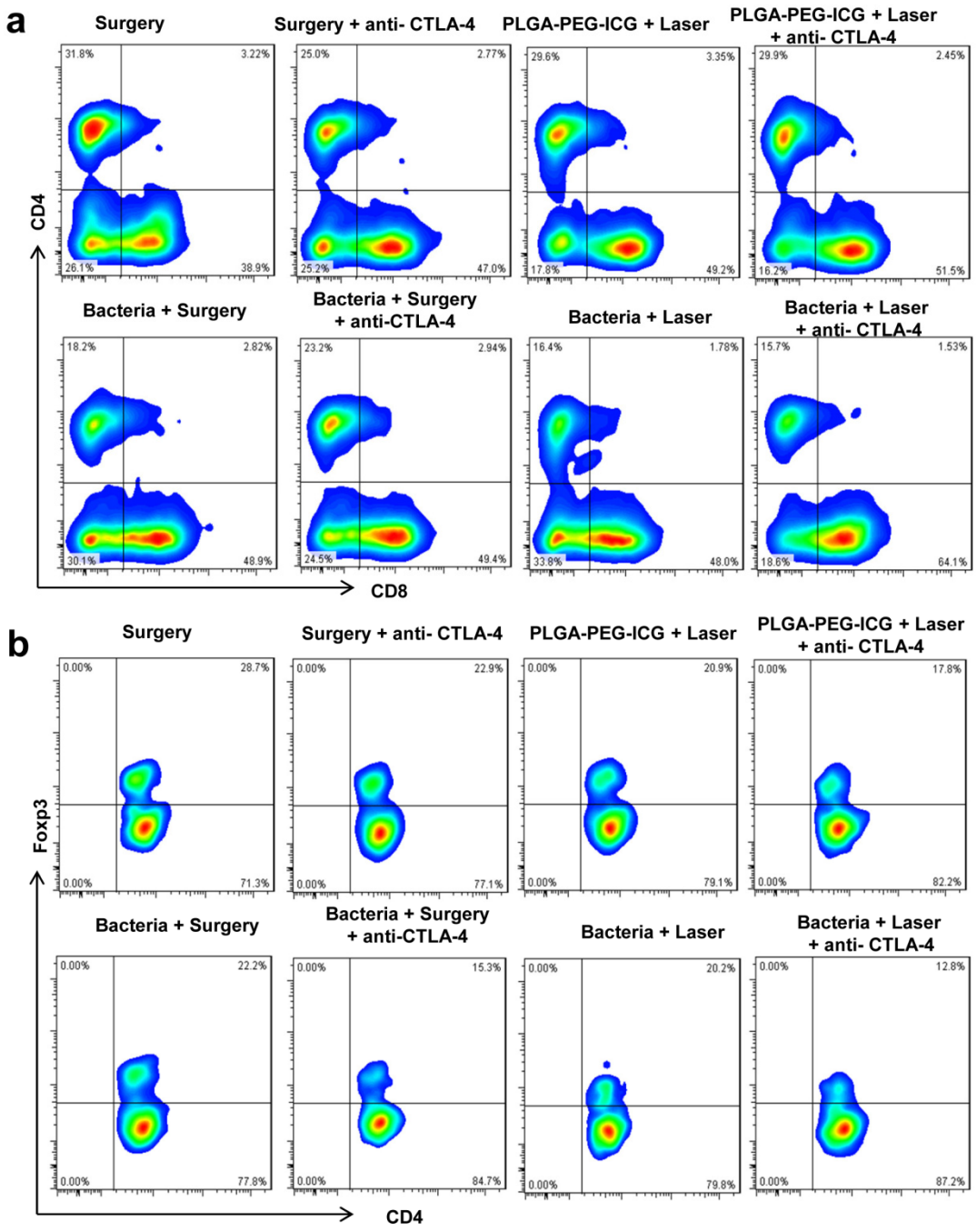

Supporting information Figure S15. Representative flow cytometry plots showing different groups of T cells and percentages (gated on CD4+cells) of CD4 + FoxP3 + T cells in secondary tumors. (a) c Tumor cell suspensions were analyzed by flow cytometry for T-cell infiltration (gated on CD3+ T cells). (b) Representative flow cytometry plots showing percentages (gated on CD4+cells) of CD4 + FoxP3 + T cells in secondary tumors after various treatments indicated.

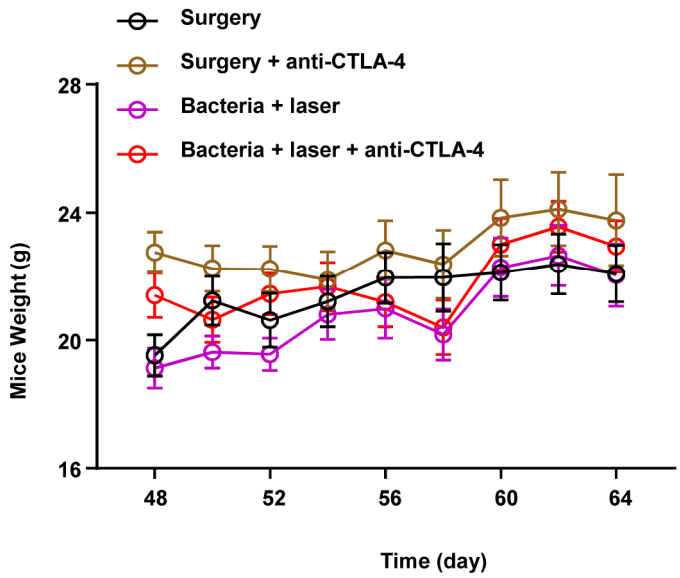

Supporting information Figure S16. Average body weights of mice in the experiment of immune-memory assessment after various treatments indicated. Five mice were used in each group.